

# Bubble Pump Design for Single Pressure Absorption Refrigeration Cycles

**Sam V. Shelton, Ph.D.**  
Fellow ASHRAE

**Susan White Stewart**  
Student Member ASHRAE

## ABSTRACT

A model has been developed for the design and optimization of a small bubble pump to be used in a single pressure absorption refrigeration cycle to lift the working fluid mixture against gravity and overcome flow friction. This analytical model is developed from two-phase flow fundamentals and incorporates the design parameters of the bubble pump. Parametric studies are carried out and a design optimization for maximum efficiency is performed for various operating conditions. Optimum efficiency is defined as the liquid pumped per unit of bubble pump heat input. The results show the optimum bubble pump tube diameter over a range of operating conditions.

## INTRODUCTION

Conventional refrigeration systems are dual pressure cycles where the saturation temperature difference between the condenser and evaporator is produced by a system pressure difference. This requires a mechanical input to drive the compressor or pump needed to generate this change in pressure, which adds significantly to the noise level and cost of the system while reducing the reliability and portability. On the other hand, single pressure absorption refrigeration systems, such as the von Platen and Munters (1928) diffusion-absorption cycle and the Einstein cycle (Einstein and Szilard 1928), use at least three working fluids to create temperature changes by imposing partial pressures on the refrigerant. While termed "single pressure," there are still slight overall pressure variations within these cycles due to flow friction and gravity. So, despite there being no need to pump the fluid to a much higher pressure to create a change in saturation temperature, a mechanism is needed to move the fluid through the cycle against

flow friction and gravity. To eliminate the need for a mechanical input, a heat-driven bubble pump is used for this purpose.

Percolating coffee makers are a well-known application of bubble pumps. Heat addition to the fluid at the base of a vertical tube creates vapor, thereby increasing the buoyancy of the fluid causing it to rise through the vertical tube under two-phase flow conditions, as seen in Figure 1.

Experimental studies were performed by White (2001) on an air-lift pump, which operates on the same principals as a

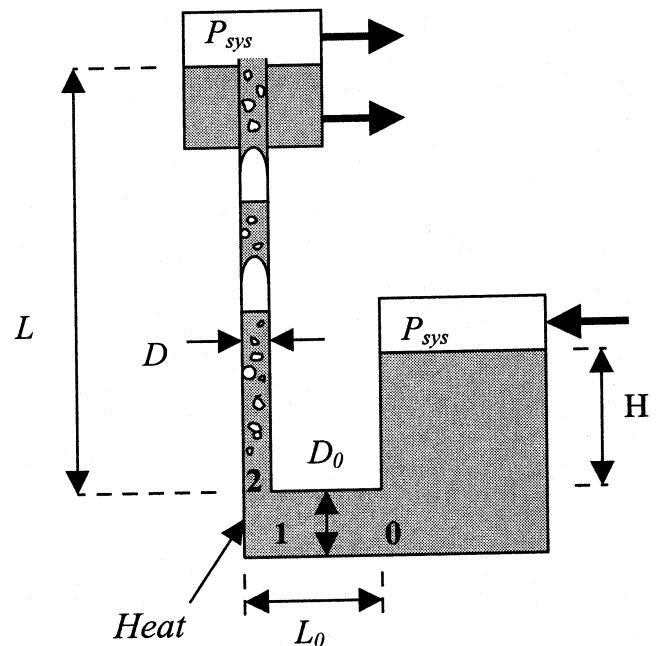
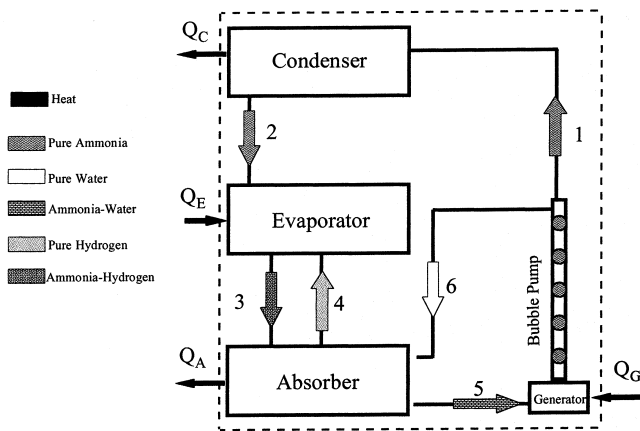


Figure 1 Bubble pump configuration.

Sam V. Shelton is an associate professor and Susan White Stewart is a graduate student, Department of Mechanical Engineering, Georgia Institute of Technology, Atlanta, Ga.



**Figure 2** Diffusion-absorption cycle.

bubble pump, and the results were compared with five different bubble pump models. All of these models used basic conservation equations to formulate the average pressure gradient along the lift tube. Four of the models used the drift flux method (Zuber and Findlay 1965) to analyze the void fraction in the lift tube and differ only by constants used in the drift velocity term (de Cachard and Delhaye 1996; Chexal et al. 1992; Reinemann et al. 1990; and Nicklin 1963). The fifth model (Delano 1998) assigns a value to the slip velocity, which is related to the void fraction, recommended by Stenning and Martin (1968).

White (2001) found that the model that showed the most consistent agreement with the experimental studies was one based on the drift flux method using the term for the drift velocity ( $V_{gi}$ ) formulated by de Cachard and Delhaye (1996). This model is used here to analyze the bubble pump component of a single pressure absorption cycle. The model is developed in an engineering equation solver (EES) (Klein and Alvarado 2000) to optimize for maximum efficiency under various operating conditions. Optimum efficiency is defined as the liquid mass pumped per unit of bubble pump heat input (kg/KJ, not on a 0-100% scale). The results show there is an optimum bubble pump tube diameter for a given set of operating conditions.

## BACKGROUND

Because of their single pressure operation, the diffusion-absorption and Einstein cycles are able to completely avoid the need for electric power, along with its associated central power plant and electric distribution infrastructure and instead rely on a direct thermal energy source. This helps avert the need to wastefully convert heat to work and then back to heat. They also use environmentally benign fluids, an increasingly important issue as several man-made refrigerants are phased out over the next few years. Additionally, they are portable, reliable, operate silently, and are inexpensive to build. However, with relatively low refrigeration COPs, they have

limited applications. When used for heating, both cycles can achieve efficiencies over 100% (Schaefer 2000). In this situation, the low COP is less of an issue when competing against direct-fired heating devices.

## Cycle Descriptions

The von Platen and Munters (1928) diffusion-absorption cycle is similar to an ammonia-water absorption cycle with an inert gas, usually hydrogen, diffused through the system to maintain a uniform system pressure throughout the cycle. Shown in Figure 2, the diffusion-absorption cycle consists of a generator, bubble pump, absorber, and condenser with ammonia, water, and hydrogen as the working fluids.

When heat is supplied to the generator (5), bubbles of ammonia gas are produced from the ammonia-water mixture. The ammonia bubbles rise and lift with the weak ammonia-water solution (weak in ammonia) through the bubble pump lift tube. The weak solution is sent to the absorber (6), while the ammonia vapor rises to the condenser (1). In the condenser, heat is removed from the ammonia vapor, causing it to condense to a liquid at the system's total pressure. The condensed ammonia flows down into the evaporator (2). Hydrogen supplied to the evaporator passes across the surface of the ammonia, lowering the partial pressure on the liquid ammonia. This reduction in the partial pressure allows the liquid ammonia to evaporate at a lower temperature. The evaporation of the ammonia extracts heat from the evaporator, providing refrigeration to the food storage space. The mixture of ammonia and hydrogen vapor falls from the evaporator to the absorber (3). A continuous trickle of weak ammonia-water solution enters the upper portion of the absorber (6). It is fed by gravity from the bubble pump. This weak ammonia-water solution absorbs the vapor ammonia leaving the light hydrogen to rise back to the evaporator (4). Finally, the strong ammonia-water solution flows back into the generator/bubble pump system (5), thus completing the cycle.

The diffusion-absorption cycle has a niche market in the recreational vehicle and hotel room refrigerator markets (Herold et al. 1996). It is manufactured in many parts of the world today. Since its invention, several attempts have been made to make it more competitive with dual-pressure cycles by improving its efficiency, but at refrigeration temperatures, a COP of approximately 0.3 is the best attained (Chen et al. 1996).

In 1928, Einstein and Szilard also patented a single pressure absorption cycle. Unlike the diffusion-absorption cycle, however, the Einstein cycle uses a pressure-equalizing absorbate fluid rather than an inert gas. In the Einstein cycle, butane is the refrigerant, water remains the absorbent, and ammonia becomes the pressure-equalizing fluid. The generator, bubble pump, and evaporator are the same as the von Platen and Munters cycle, but the condenser and absorber are combined into a single unit. It also operates at a single system pressure. In the evaporator, the partial pressure on the entering liquid butane is reduced by ammonia vapor, allowing it to evaporate at a lower temperature. In the condenser/absorber, the partial pressure of the butane vapor coming from the evaporator is

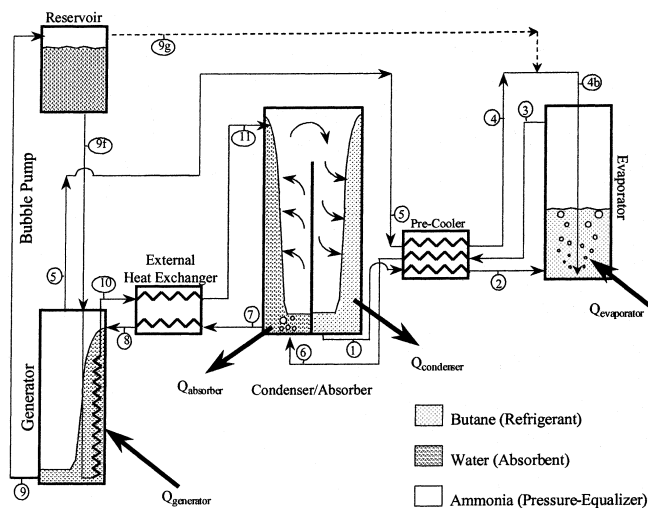


**Figure 3** The Einstein refrigeration cycle.

increased when the ammonia vapor is absorbed by liquid water, thus allowing the butane to condense at a higher temperature. The liquid butane and liquid ammonia-water naturally separate due to their respective density differences and the fact that ammonia-water is immiscible with butane at the condenser/absorber's temperature and pressure. The ammonia is then separated from the water in a generator by the application of heat.

Delano (1998) performed a design analysis of the cycle and added two regenerative heat exchangers to improve efficiency. These include an internal regenerative heat exchanger in the generator and an evaporator pre-cooler. This cycle schematic can be seen in Figure 3.

While early models predicted the cycle's cooling COP to be about 0.4, more recent studies have shown it to be about 0.2 (Shelton et al. 1999), which is relatively low compared to the thermal efficiency of dual pressure refrigeration cycles but competitive with the diffusion-absorption cycle. One advantage of the Einstein cycle is its use of a different generator absorbate, ammonia, than that used in the evaporator, butane. This decouples the temperature difference between the generator/condenser and the condenser/evaporator.

## Literature Review

Recently there has been a lot of interest in the diffusion-absorption cycle. Herold et al. (1996) gives a review of the details of its operation and performance. Chen et al. (1996) investigated the diffusion-absorption cycle for enhancing its performance. The result was a new design for the bubble pump/generator configuration. The original design had combined the generator and the bubble pump into one component, with only one heat addition. The modified version heats the strong ammonia solution first, extracting most of the ammonia from the water so that a weak ammonia solution is sent to the bubble pump where another heater causes the solu-

tion to boil and rise, due to increased buoyancy, through the lift tube. This design is virtually identical to the bubble pump/generator configuration in the Einstein cycle; therefore, the same bubble pump model can be used for both cycles.

Chen et al. (1996) experimentally found that this new configuration increased the COP by about 50%; however, a detailed theoretical model was not developed in this publication. Earlier, Hassoon (1989) provided a theoretical model and experimental results for a bubble pump that uses injected steam for lift instead of vaporizing the liquid in the tube. However, it modeled a lift tube that was cooled along its length.

In 1998, Delano modeled the bubble pump of the Einstein cycle and analyzed its performance. Schaeffer (2000) uses the same analysis as Delano but with a two-phase friction factor. In addition, Schaeffer analyzed the relationship of diameter, submergence ratio, mass flow rate, and heat input to maximize performance. Sathe (2001) also uses Delano's (1998) analysis except in reference to a diffusion-absorption cycle. These bubble pump models are based on an air-lift pump analysis by Stenning and Martin (1968).

Air-lift pumps operate on the same principals as bubble pumps except that air is injected to increase the buoyancy of the fluid instead of bubbles forming from liquid vaporization. There is much more information available in the literature on air-lift pumps than bubble pumps (Stepanoff 1929; Pickert 1932; White and Beardmore 1962; Nicklin 1963; Zukoski 1966; Stenning and Martin 1968; Todoroki et al. 1973; Kouremenos and Staicos 1985; Clark and Dabolt 1986; Reinemann et al. 1990; de Cachard and Delhaye 1996).

Air-lift pumps have a wide variety of applications. The earlier studies have been concerned with dewatering mines or raising oil from dead wells and, therefore, analyze pumps with a much larger lift length and diameter than those applicable to the current study. More recently, the importance of air-lifts in moving liquids at nuclear fuel reprocessing plants has been realized, requiring more accurate design equations (Clark and Dabolt 1986). However, the point to which they explore the two-phase flow details in the lift tube to obtain the frictional pressure drop is beyond the scope of this study. Certain assumptions have been made in the current study to simplify the model considerably, without risking significant degradation in accuracy for small-scale bubble pumps (Clark and Dabolt 1986).

Both bubble pumps (also called vapor-lift pumps) and air-lift pumps are essentially two-phase flow in a vertical pipe and therefore, can be modeled by two-phase flow theories. Chisholm (1983) provides a good starting point for understanding the basic definitions and flow patterns encountered in two-phase flows. In essence, two-phase flow is a mixture of either a vapor and a liquid, or a gas and a liquid, moving through a pipe. The four basic flow patterns observed in vertical two-phase flows: bubbly, slug, churn, and annular, as shown in Figure 4 (Collier and Thome 1996). However, the exact definitions of patterns vary by author, and flows are sometimes described as a combination of patterns. Some of the terminology associated with two-phase flow is shown in Table 1.

**TABLE 1**  
**Two-Phase Flow Parameters**

Parameter	Units (SI)	Units (I-P)	Definition
$\rho_G$	kg/m <sup>3</sup>	lb <sub>m</sub> /in. <sup>3</sup>	Density of gas phase
$\rho_L$	kg/m <sup>3</sup>	lb <sub>m</sub> /in. <sup>3</sup>	Density of liquid phase
$D$	m	in.	Diameter of lift tube
$A = \pi D^2/4$	m <sup>2</sup>	in. <sup>2</sup>	Total cross sectional area of pipe
$A_G$	m <sup>2</sup>	in. <sup>2</sup>	Cross sectional area gas occupies
$A_L = A - A_G$	m <sup>2</sup>	in. <sup>2</sup>	Cross sectional area liquid occupies
$\varepsilon = A_G/A$	-	-	Gas void fraction of the flow
$\dot{V}_G$	m <sup>3</sup> /s	ft <sup>3</sup> /s	Gas volumetric flow rate
$\dot{V}_L$	m <sup>3</sup> /s	ft <sup>3</sup> /s	Liquid volumetric flow rate
$\dot{V} = \dot{V}_L + \dot{V}_G$	m <sup>3</sup> /s	ft <sup>3</sup> /s	Total volumetric flow rate
$j_G = \dot{V}_G/A$	m/s	ft/s	Gas superficial velocity
$j_L = \dot{V}_L/A$	m/s	ft/s	Liquid superficial velocity
$j = j_L + j_G$	m/s	ft/s	Total average velocity of flow
$V_G = j_G/\varepsilon$	m/s	ft/s	Velocity of the gas
$V_L = j_L/(1-\varepsilon)$	m/s	ft/s	Velocity of the liquid
$\dot{m}_G$	kg/s	lb <sub>m</sub> /s	Mass flow rate of gas
$\dot{m}$	kg/s	lb <sub>m</sub> /s	Total mass flow rate
$x = \dot{m}_G/\dot{m}$	-	-	Quality
$S = V_G/V_L$	-	-	Slip between phases

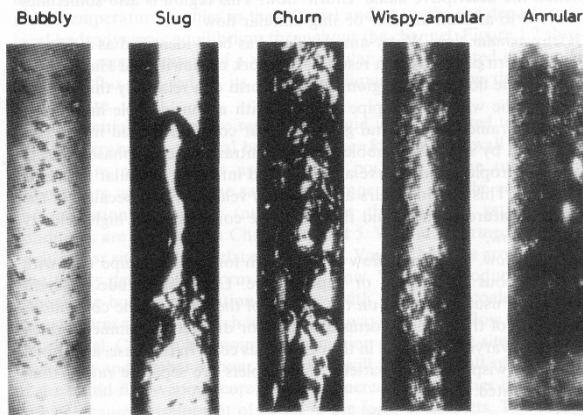


**Figure 4** Vertical two-phase flow regimes.

## MODEL

The drift-flux model is the widely accepted method for analyzing void fractions in two-phase flow. This method, formalized by Zuber and Findlay in 1965, provides a means to account for the effects of the local relative velocity between the phases as well as the effects of non-uniform phase velocity and concentration distributions.

While many others contributed to the beginnings of two-phase flow theory, Zuber and Findlay's (1965) analysis estab-

lishes the basis of the drift flux formulation used today (Chexal et al. 1997). It relates the average gas void fraction of the two-phase flow to (1) the superficial velocities,  $j$ , of the gas and liquid phases (the velocity each phase would have if it occupied the entire cross sectional flow area of the pipe alone); (2) the distribution parameter,  $C_0$ ; and (3) the drift velocity,  $V_{gj}$  ( $= V_G - j$ ). The resulting drift flux model can be summarized by the following equation:

$$\varepsilon = \frac{j_G}{C_0(j_L + j_G) + V_{gj}} \quad (1)$$

Correlations for  $C_0$  and  $V_{gj}$  have been empirically formulated for the different two-phase vertical flow regimes shown in Figure 3. The constants which White (2001) found best-fit experimental data (for the slug regime) were given by de Cachard and Delhaye (1996) as:

$$C_0 = 1.2 \quad (2)$$

$$V_{gj} = 0.345(1 - e^{-0.01N_f/0.345})[1 - e^{(3.37 - Bo)/m}]\sqrt{gD} \quad (3)$$

where

$$(N_f)^2 = \frac{\rho_L(\rho_L - \rho_G)gD^3}{\mu_L^2} \quad (4)$$

Bond number:

$$Bo = \frac{(\rho_L - \rho_G)gD^2}{\sigma} \quad (5)$$

$$m = 10 \quad \text{when} \quad N_f > 250 \quad (6a)$$

$$m = 69(N_f)^{-0.35} \quad \text{when} \quad 18 < N_f < 250 \quad (6b)$$

$$m = 25 \quad \text{when} \quad N_f < 18 \quad (6c)$$

## Two-Phase Properties

One issue in modeling two-phase flow is in defining two-phase friction factors and properties of the mixture. These are needed in the governing equations. Lockhart and Martinelli (1949) defined a two-phase multiplier, used with a single-phase pressure drop calculation. Beattie and Whalley (1982) recommend using the Colebrook equation for friction using two-phase properties in the Reynolds number derived from a homogeneous model, which models a single phase flow at the average properties of the individual phases:

$$\frac{1}{\sqrt{f_{TP}}} = 3.48 - 4 \log_{10} \left[ 2 \frac{\varepsilon_R}{D} + \frac{9.35}{Re_{TP} \sqrt{f_{TP}}} \right] \quad (7)$$

where the parameters are defined as follows:

Fanning friction factor:

$$f_{TP}^* = f_{TP}/4 \quad (8)$$

Pipe roughness (m):

$$\varepsilon_R$$

Two-phase Reynolds number:

$$Re_{TP} = \frac{\rho_G j_G + \rho_L j_L}{\mu_{TP}} \quad (9)$$

Two-phase viscosity (kg/m·s):

$$\mu_{TP} = \varepsilon_h \mu_G + \mu_L (1 - \varepsilon_h) (1 + 2.5 \varepsilon_h) \quad (10)$$

Homogeneous void fraction (when slip,  $S$ , is 1):

$$\varepsilon_h = \frac{x}{x + \frac{\rho_L}{\rho_G} (1 - x)} \quad (11)$$

## Governing Equations

The submergence ratio of the bubble pump, which describes the average pressure gradient along the lift tube, can be solved for in terms of velocities, geometrical parameters, and fluid properties by using momentum and mass balances. The following equations are based on Figure 1. Minor frictional losses in the entrance to the lift tube have been neglected.

Momentum equation from  $P_{sys}$  to 0 gives:

$$P_0 = P_{sys} + \rho_L g H - \rho_L \frac{V_0^2}{2} \quad (12)$$

where

$V_0$  = the velocity (m/s) at state 0 (liquid solution)

Momentum equation from 0 to 1 yields (neglecting friction):

$$P_1 = P_0 - \rho_L V_0 (V_1 - V_0) \quad (13)$$

where

$V_1$  = the velocity (m/s) at state 1 (two phase flow)

$D_0$  = the diameter (m) of the water entrance line

$L_0$  = the length (m) of the water entrance line

$f_L$  = the friction factor in the water entrance line

Conservation of mass with constant density and area from 0 to 1 yields:

$$V_0 = V_1 \quad (14)$$

Conservation of momentum from state 1 to 2, neglecting friction in this small region:

$$P_2 = P_1 - \rho_2 V_1 (V_2 - V_1) \quad (15)$$

The conservation of mass from state 1 to 2 is

$$\rho_1 A_0 V_1 = \rho_2 A_2 V_2. \quad (16)$$

Therefore,

$$\rho_2 = \frac{\rho_L V_1}{V_2}. \quad (17)$$

Momentum equation from state 2 to  $P_{sys}$ :

$$P_2 = P_{sys} + f_{TP} \frac{\rho_2 V_2^2}{2} \left( \frac{L}{D} \right) + \frac{\rho_L L g A_L}{A} \quad (18)$$

where

$f_{TP}$  = the two-phase friction factor (based on average properties of liquid and gas).

A general equation for the submergence ratio ( $H/L$ ), which describes the average pressure gradient along the lift tube, can be developed by combining Equations 12, 13, 15, and 18.

$$\frac{H}{L} = \frac{f_{TP} \rho_2 V_2^2}{2 \rho_L g D} + \frac{A_L}{A} + \frac{V_1^2}{2 g L} + \frac{\rho_2 V_1 (V_2 - V_1)}{\rho_L g L} \quad (19)$$

Now, from the definitions of superficial velocities and void fraction, this relationship can be related to two-phase flow parameters (see Table 1 for definitions). Since states 0 and 1 are at liquid conditions,

$$V_0 = V_1 = \frac{\dot{V}_L}{A_0}, \quad (20)$$

while the definition of  $j_L$  is

$$j_L = \frac{\dot{V}_L}{A}. \quad (21)$$

Therefore,

$$V_0 = V_1 = j_L \left( \frac{A}{A_0} \right) \quad (22)$$

Additionally, state 2 has two phases, but  $V_2$  still describes the total average velocity of the mixture:

$$V_2 = \frac{\dot{V}_L + \dot{V}_G}{A} = \frac{\dot{V}}{A}, \quad (23)$$

which is precisely the definition of  $j$ . Therefore,

$$V_2 = j. \quad (24)$$

It follows from Equations 24 and 26 that

$$V_2 - V_1 = j - j_L \left( \frac{A}{A_0} \right). \quad (25)$$

Also, the void fraction is defined as the cross-sectional area occupied by the gas divided by the total cross-sectional area of the pipe. Therefore,

$$\frac{A_L}{A} = \frac{A - A_G}{A} = 1 - \epsilon. \quad (26)$$

Using Equations 17, 22, 24, 25, and 26 in Equation 19,

$$\frac{H}{L} = \frac{f_{TP} j^2 \rho_2}{2gD\rho_L} + \frac{j_L^2 \left( \frac{D}{D_0} \right)^4}{2gL} + \frac{j_L^2 \rho_L \left( \frac{D}{D_0} \right)^4 \left( j - j_L \left( \frac{D}{D_0} \right)^2 \right)}{\rho_L g L} + (1 - \epsilon). \quad (27)$$

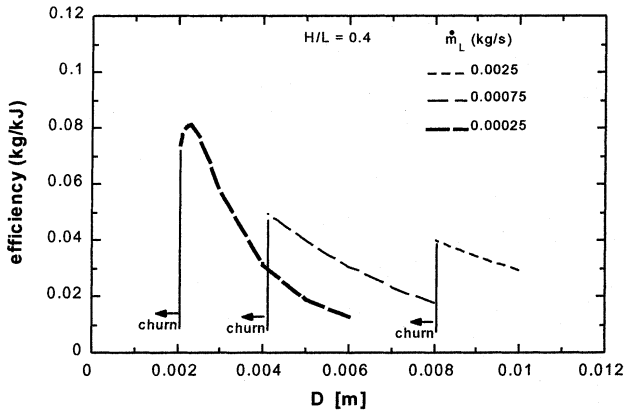


Figure 5a Efficiency vs. diameter,  $H/L = 0.4$  (SI).

This equation is used to model the average pressure gradient along the bubble pump lift tube.

## RESULTS AND DISCUSSION

The system temperature and pressure used for calculations were 375 K (215.3°F) and 4 bars (58 psi), respectively, while the fluid used was an ammonia-water mixture of 15.5% ammonia concentration. These values were determined by the generator outlet conditions from Delano's (1998) base case design of the Einstein cycle. Properties of the ammonia-water mixture other than surface tension and viscosity were found using the thermophysical property functions in EES. The surface tension of the ammonia-water mixture was found in IIR (1994) to be 0.043 N/m (0.0029  $\text{lb}_f/\text{ft}$ ) under the prescribed system pressure and concentration. The solution viscosity was also found in IIR (1994) as 0.0003  $\text{kg}/\text{m}\cdot\text{s}$  ( $6.26 \times 10^{-6} \text{lb}_f\cdot\text{s}/\text{ft}^2$ ).

The submergence ratio and the mass flow rate of the liquid were varied to find their respective importance, while the length of the lift tube was set as 0.5 m (1.64 ft). Additionally, the diameter of the entrance line ( $D_0$ ) was set equal to the diameter of the lift tube ( $D$ ). Finally, the tube diameter varied between about 2 mm and 20 mm (0.08 in. and 0.8 in.) depending on where the maximum efficiency, defined as the liquid mass flow rate pumped per unit of heat input to the bubble pump ( $\dot{m}_L/\dot{Q}_{BP}$ ), and was found for each case. Efficiency was plotted versus the diameter to find the optimum lift tube diameter. The resulting plots are shown in Figures 5 through 7.

The range of liquid mass flow rates used in the study was taken around the base case of Delano's (1998) design for an evaporator refrigerating capacity chosen as 100 W (341.2 Btu/h). That study found the required bubble pump liquid flow rate for this size system is 0.00075  $\text{kg}/\text{s}$  (0.00165  $\text{lb}_m/\text{s}$ ). In order to obtain a range of values, liquid mass flow rates of 0.00025  $\text{kg}/\text{s}$  ( $5.51 \times 10^{-4} \text{lb}_m/\text{s}$ ) and 0.0025  $\text{kg}/\text{s}$  (0.00551  $\text{lb}_m/\text{s}$ ) were also used.

It was found that the results were not sensitive to the length of the tube as long as it remained short, under approximately 2 m (6 ft). The more important parameter is the submergence ratio. As can be seen from Figures 5, 6, and 7, the efficiency range is drastically different for the various values

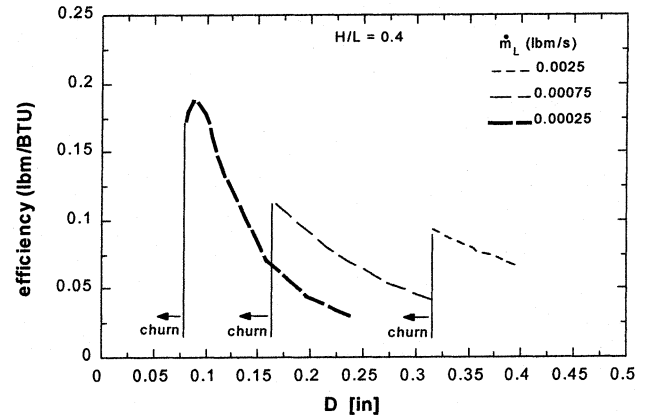


Figure 5b Efficiency vs. diameter,  $H/L = 0.4$  (IP).

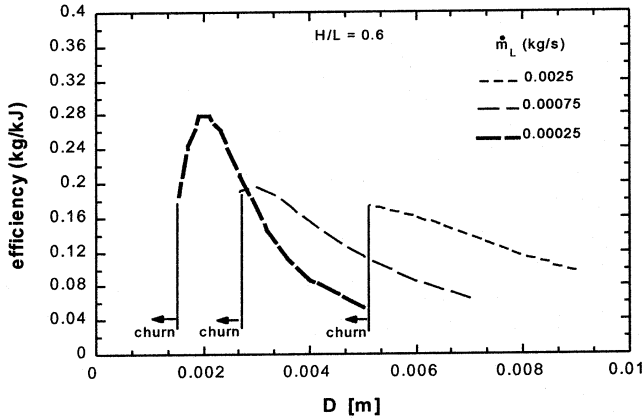


Figure 6a Efficiency vs. diameter,  $H/L = 0.6$  (SI).

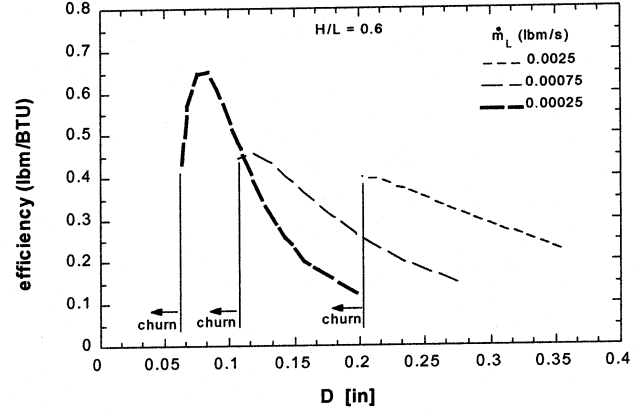


Figure 6b Efficiency vs. diameter,  $H/L = 0.6$  (I-P).

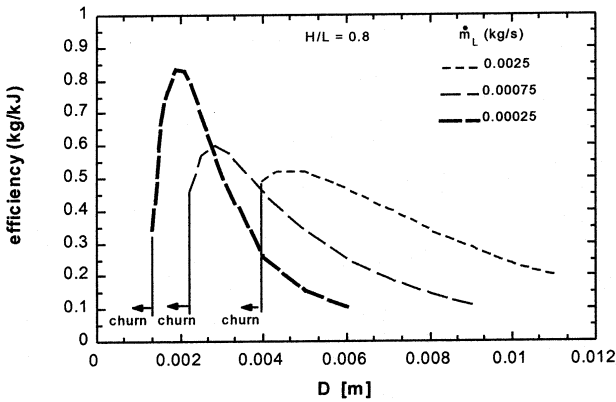


Figure 7a Efficiency vs. diameter,  $H/L = 0.8$  (SI).

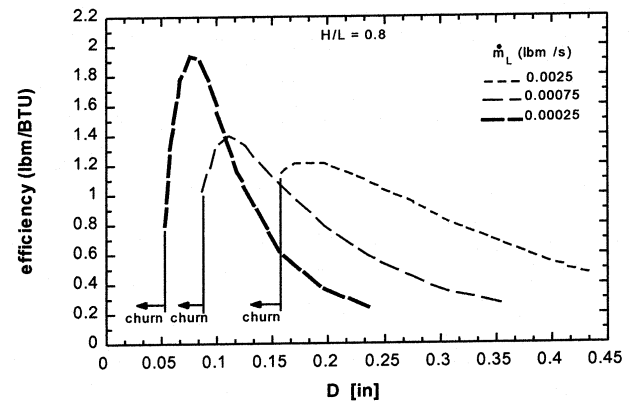


Figure 7b Efficiency vs. diameter,  $H/L = 0.8$  (I-P).

of  $H/L$ . This makes sense, since if the submergence ratio was increased to one, no ammonia gas would be needed to increase the buoyancy of the liquid mixture as the fluid would be able to reach the top of the lift tube by its own weight acting down in the generator. Therefore, the mass flow rate of gas would be zero, making the bubble pump heat input zero, causing the ratio to go to infinity. Different values of  $H/L$  are plotted (0.4, 0.6, and 0.8) to show these effects. Therefore, to obtain the highest efficiency for any design, the submergence ratio should always be maximized.

In Figures 5 through 7, it can be seen that there is an optimum diameter for a specific liquid mass flow rate and submergence ratio. White (2001) found in her experimental studies that the peak of the efficiency curve is very close to the transition from slug to churn flow. However, the de Cachard and Delhaye (1996) slug flow model is not applicable to churn flow and the efficiency falls dramatically when transition to churn flow occurs. Therefore, in order to find the optimum diameter for a given operating condition, a transition criterion must be used as a limiting factor.

Jayanti and Hewitt (1992) reviewed four models for predicting the transition from slug to churn flow in vertical tubes. They concluded that the slug to churn transition is attributed to the flooding of the liquid film surrounding the

Taylor bubble in slug flow. McQuillan and Whalley (1985), Nicklin and Davidson (1962), Wallis (1969), and Govan et al. (1991) also came to this conclusion. Flooding is manifested by the onset of upward liquid flow in the countercurrent flow of a falling liquid film and an upward-flowing gas stream. This situation occurs inside the Taylor bubble in slug flow and the slug/churn transition is reached when the fluid velocities are such that flooding occurs (Watson and Hewitt 1999).

One method for the prediction of the flooding velocity is the following semi-empirical equation proposed by Wallis (1961) and Hewitt and Wallis (1963):

$$\sqrt{j_G^*} + \sqrt{j_L^*} = \text{Constant} \quad (28)$$

where  $j_G^*$  and  $j_L^*$ , the non-dimensionalized gas and liquid superficial velocities, are defined as

$$j_G^* = j_G \frac{\sqrt{\rho_G}}{\sqrt{gD(\rho_G - \rho_L)}} \quad \text{and} \quad j_L^* = j_L \frac{\sqrt{\rho_L}}{\sqrt{gD(\rho_L - \rho_G)}} \quad (29)$$

However, Jayanti and Hewitt concluded that this model does not account for the effect of length of the falling film on the flooding velocity. To correct this, they suggest using

$$\sqrt{j_G^*} + m\sqrt{j_L^*} = \text{Constant}, \quad (30)$$

where

$$m = 0.1928 + 0.01089\left(\frac{L}{D}\right) - 3.754 \times 10^{-5}\left(\frac{L}{D}\right)^2 \quad (31)$$

$$\text{if } \frac{L}{D} \leq 120$$

$$m = 0.96 \quad \text{if } \frac{L}{D} > 120 \quad (32)$$

The constant in Equation 30 is said to be 0.75 for sharp flanges into the tube, 0.88 for rounded flanges, and a value of unity for smooth inlet and outlet conditions (Jayanti and Hewitt 1992). In White's (2001) study, a value of approximately 0.83 proved to be a very good predictor of the slug-churn transition. Therefore, the following limitation, Equation 33, should be used as a constraint of the slug flow bubble pump model, with the optimum operating condition occurring at or below the point where the right hand side value is approximately 0.83. Beyond this value, transition to churn flow diminishes the bubble pump's efficiency.

$$\sqrt{j_G^*} + m\sqrt{j_L^*} < 0.83 \quad (33)$$

In Figures 5 through 7, the slug/churn transition diameter is shown for each liquid mass flow rate value. To the left of the line, the flow is in the churn regime, therefore, the slug flow model is not valid. Hence, the optimum operating condition will be at the maximum efficiency on the curve to the right of the transition line for a given liquid mass flow rate and submergence ratio.

## CONCLUSIONS AND RECOMMENDATIONS

One of the greatest benefits of single pressure absorption refrigeration cycles is that they do not need a mechanical input. Due to their low head requirement, they can utilize a thermally driven bubble pump instead of a compressor or solution pump. However, the thermal requirement of the bubble pump can be very significant compared to the generator, reducing the thermal efficiency of the single pressure absorption cycle. Therefore, this bubble pump heat input should be minimized.

The current study found there is an optimum diameter, ranging from 2 mm (0.079 in.) to 6 mm (0.236 in.) for a required liquid pumping rate of 0.00025 kg/s (0.000551 lb<sub>m</sub>/s) to 0.0025 kg/s (0.00551 lb<sub>m</sub>/s), for maximizing the efficiency of the bubble pump component. However, the efficiency rapidly decreases when diameters smaller than the optimum value are used. Therefore, it is recommended to use a slightly larger diameter than the optimum value.

The peak efficiency values for the cases studied ranged from a low of about 0.05 kg/kJ (0.1163 lb<sub>m</sub>/Btu) for a required liquid flow of 0.0025 kg/s (0.00551 lb<sub>m</sub>/s) and submergence ratio of 0.4, to a high of about 1.0 kg/kJ (2.326 lb<sub>m</sub>/Btu) for a required liquid flow of 0.00025 kg/s (0.000551 lb<sub>m</sub>/s) and

submergence ratio of 0.8. The optimum efficiency value is most sensitive to the submergence ratio, changing by a factor of about ten as the submergence changes from 0.4 to 0.8 at a fixed liquid flow rate. Changing the liquid flow rate at fixed submergence ratio has a lesser effect, changing the efficiency by about a factor of two as the flow rate is varied by a factor of three.

For fixed submergence ratio and liquid flow rate, there is a rapid drop in efficiency as the diameter drops below some value. This rapid drop off is due to the transition from slug to churn flow. Therefore, a limiting lower diameter value should be set to stay out of the churn flow regime and remain in the slug regime. The optimum efficiency diameter occurs while operating in the slug regime (White 2001), and at many operating conditions studied here, it occurs at a point just above the slug to churn transition diameter. If the calculated peak efficiency predicted by the two-phase model occurs in the churn regime, the bubble pump should be designed at a larger diameter so that it operates in the slug flow regime. This flow transition can be predicted by Equation 33. If the right-hand side is less than 0.83, then the flow will be in the slug flow regime.

It should be noted that this model is not expected to be very accurate below diameters of approximately 4 mm (0.157 in.) due to the increasing influence of surface tension in that range. It is suggested that in future studies the effects of surface tension at very small diameters be more accurately accounted for in the analysis.

## NOMENCLATURE

$A$	= cross-sectional area (m <sup>2</sup> )
$Bo$	= Bond number
$C_o$	= distribution parameter
$D$	= diameter of lift tube (m)
$D_o$	= diameter of entrance tube (m)
$f$	= friction factor
$f'$	= Fanning friction factor
$g$	= acceleration of gravity (m/s <sup>2</sup> )
$H$	= height of generator liquid level (m)
$j$	= superficial velocity (m/s)
$j^*$	= non-dimensional superficial velocity
$L$	= length of lift tube (m)
$L_o$	= length of entrance tube (m)
$m$	= constant (different in drift flux analysis than in slug/churn transition analysis)
$\dot{m}$	= mass flow rate (kg/s)
$N_f$	= viscous effects parameter
$P$	= pressure (bars)
$\dot{V}$	= volumetric flow rate (m <sup>3</sup> /s)
$Re$	= Reynolds number
$S$	= slip between phases of two-phase flow
$V$	= velocity (m/s)
$x$	= quality

## Greek letters

$\alpha$	= submergence ratio
$\varepsilon$	= void fraction
$\varepsilon_R$	= pipe roughness (m)
$\rho$	= density (kg/m <sup>3</sup> )
$\mu$	= fluid viscosity (kg/m-s)
$\sigma$	= surface tension (N/m)

### Subscripts

0	= state 0
1	= state 1
2	= state 2
<i>a</i>	= ammonia
<i>BP</i>	= bubble pump
<i>G</i>	= gas
<i>gj</i>	= drift
<i>h</i>	= homogeneous conditions
<i>L</i>	= liquid
<i>m</i>	= mixture
<i>sys</i>	= system
<i>TP</i>	= two-phase
<i>w</i>	= water

### REFERENCES

- Beattie, D.R.H., and P.B. Whalley. 1982. A simple two-phase frictional pressure drop calculation method. *Int. J. of Multiphase Flow* 8: 83-87.
- Chen, J., K.J. Kim, and K.E. Herold. 1996. Performance enhancement of a diffusion-absorption refrigerator. *Int. J. Refrig.* 19(3): 208-218.
- Chexal, B., G. Lellouche, J. Horowitz, and J. Healzer. 1992. A void fraction correlation for generalized applications. *Progress in Nuclear Energy* 27(4): 255-295.
- Chexal, B., M. Merilo, M. Maulbetsch, J. Horowitz, J. Harrison, J. Westacott, C. Peterson, W. Kastner, and H. Schmidt. 1997. *Void fraction technology for design and analysis*. Palo Alto, Calif.: Electric Power Research Institute.
- Chisholm, D. 1983. *Two-phase flow in pipelines and heat exchangers*. New York: George Goodwin.
- Clark, N.N., and R.J. Dabolt. 1986. A general design equation for air lift pumps operating in slug flow. *AICHE Journal* 32(1): 56-64.
- Collier, J.G., and J.R. Thome. 1996. *Convective boiling and condensation*. New York: McGraw-Hill Book Co.
- Delano, A. D. 1998. *Design analysis of the Einstein refrigeration cycle*. Ph.D. dissertation, Georgia Institute of Technology.
- de Cachard, F., and J.M. Delhaye. 1996. A slug-churn model for small-diameter airlift pumps. *Int. J. Multiphase Flow* 22(4): 627-649.
- Einstein, A., and L. Szilard. 1928. Improvements relating to refrigerating apparatus. (Appl. U.K. Patent: 16 Dec. 1927; Priority: Germany, 16 Dec. 1926)
- Govan, A.H., G.F. Hewitt, H.J. Richter, and A. Scott. 1991. Flooding and churn flow in vertical pipes. *Int. J. Multiphase Flow* 17: 27-44.
- Hassoon, H. 1989. A two-phase investigation relating to circulating bubble absorbers. Ph.D. thesis, Mechanical Engineering Department, University of Bristol, U.K.
- Herold, K.E., R. Radermacher, and S.A. Klein. 1996. *Absorption chillers and heat pumps*. Boca Raton, Fla.: CRC Press.
- Hewitt, G.F., and G.B. Wallis. 1963. Flooding and associated phenomena in falling film flow in a vertical tube. *UKAEA Report No. AERE-R4022*. HMSO, London.
- IIR. 1994. *Thermodynamic and physical properties of NH<sub>3</sub>-H<sub>2</sub>O*. International Institute of Refrigeration.
- Jayantani, S., and G.F. Hewitt. 1992. Prediction of slug-to-churn flow transition in vertical two-phase flow. *Int. J. Multiphase Flow* 18(6): 847-860.
- Klein, S.A., and F.L. Alvarado. 2000. Engineering equation solver. *F-Chart Software*, Ver.6.036.
- Kouremenos, D.A., and J. Staicos. 1985. Performance of a small air-lift pump. *Int. J. Heat Fluid Flow* 6: 217-222.
- Lockhart, R.W., and R.C. Martinelli. 1949. Proposed correlation of data for isothermal two-phase, two-component flow in pipes. *Chem. Eng. Prog.* 45: 39-48.
- McQuillan, K.W. and P.B. Whalley. 1985. Flow patterns in vertical two-phase flow. *Int. J. Multiphase Flow* 11: 161-175.
- Nicklin, D.J. 1963. The air-lift pump: Theory and optimization. *Trans. Instn. Chem. Engrs.* 41: 29-39.
- Nicklin, D.J., and J.F. Davidson. 1962. The onset of instability in two-phase slug flow. Presented at a *Symp. on Two-phase flow*, Inst. Mech. Engrs. London, paper no 4.
- Pickert, F. 1932. The theory of the air-lift pump. *Engineering* 34: 19-20.
- von Platen, B.C., and C.G. Munters. 1928. Refrigerator. U.S. Patent 1,685,764.
- Reinemann, D.J., J.Y. Parlange, and M.B. Timmons. 1990. Theory of small-diameter airlift pumps. *Int. J. Multiphase Flow* 16: 113-122.
- Sathe, A. 2001. *Experimental and theoretical studies on a bubble pump for a diffusion absorption refrigeration system*. Master of technology project report, Universitat Stuttgart.
- Schaefer, L.A. 2000. *Single pressure absorption heat pump analysis*. Ph.D. dissertation, Georgia Institute of Technology.
- Shelton, S., A. Delano, and L. Schaefer. 1999. Second law study of the Einstein refrigeration cycle. *Proceedings of the Renewable and Advanced Energy Systems for the 21st Century*, April 1999.

- Stenning, A., and C. Martin. 1968. An analytical and experimental study of air-lift pump performance. *ASME Journal of Engineering for Power*, pp. 106-110.
- Stepanoff, A.J. 1929. Thermodynamic theory of the air lift pump. *ASME Transactions* 51: 49-55.
- Todoroki, I., S. Yoshifusa, and T. Honda. 1973. Performance of air-lift pump. *Bulletin of ASME* 16: 733-741.
- Wallis, G.B. 1961. Flooding velocities for air and water in vertical tubes. *UKAEA Report No. AEEW-R123*. HMSO, London.
- Wallis, G.B. 1969. *One-dimensional two-phase flow*. New York: McGraw-Hill.
- Watson, M.J., and G.F. Hewitt. 1999. Pressure effects on the slug to churn transition. *Int. J. of Multiphase Flow* 25: 1225-1241.
- White, E.T., and R.H. Beardmore. 1962. The velocity of rise of single cylindrical air bubbles through liquids contained in vertical tubes. *Chem. Engng Sci.* 17: 351-361.
- White, S.J. 2001. *Bubble pump design and performance*. Master's thesis, Georgia Institute of Technology.
- Zuber, N., and J. Findlay. 1965. Average volumetric concentration in two-phase flow systems. *J. of Heat Transfer* 87: 453-468.
- Zukoski, E.E. 1966. Influence of viscosity, surface tension, and inclination angle on motion of long bubbles in closed tubes. *J. Fluid Mech.* 20: 821-832.